Published in final edited form as:
J Invest Dermatol. 2011 February ; 131(2): 311–319. doi:10.1038/jid.2010.296.

Activated Kras Alters Epidermal Homeostasis of Mouse Skin, Resulting in Redundant Skin and Defective Hair Cycling

Anandaroop Mukhopadhyay[1,2], **Suguna R. Krishnaswami**[1,2], and **Benjamin D.-Y. Yu**[1]
[1]Division of Dermatology, Department of Medicine, UCSD Stem Cell Program, and Institute for Genomic Medicine, University of California, San Diego, San Diego, California, USA

Abstract

Germline mutations in the RAS–mitogen-activated protein kinase (RAS/MAPK) pathway are associated with genodermatoses, characterized by cutaneous, cardiac, and craniofacial defects, and cancer predisposition. Whereas activating mutations in HRAS are associated with the vast majority of patients with Costello syndrome, mutations in its paralog, KRAS, are rare. To better understand the disparity among RAS paralogs in human syndromes, we generated mice that activate a gain-of-function *Kras* allele (*Lox-Stop-Lox* (*LSL*)-*Kras^{G12D}*) in ectodermal tissue using two different Cre transgenic lines. Using Msx2-Cre or ligand-inducible keratin 15 (K15)-*CrePR*, the embryonic effects of activated Kras were bypassed and the effects of *Kras^{G12D}* expression from its endogenous promoter were determined. We found that *Kras^{G12D}* induced redundant skin, papillomas, shortened nails, and hair loss. Redundant skin was associated with basal keratinocyte hyperplasia and an increase in body surface area. Paradoxically, *Kras^{G12D}* also prevented hair cycle activation. We find that *Kras^{G12D}* blocks proliferation in the bulge region of the hair follicle, when activated through Msx2-*Cre* but not through K15-*CrePR*. These studies reveal that KRAS, although infrequently involved in RAS/MAPK syndromes, is capable of inducing multiple cutaneous features that grossly resemble human RAS/MAPK syndromes.

INTRODUCTION

RAS–mitogen-activated protein kinase (RAS/MAPK) proteins link extracellular growth factor signals to an internal cascade of downstream pathways. Activation of RAS can be modulated at many levels, including amount and availability of ligands, receptors, adaptors, and downstream effectors (Reuther and Der, 2000; Schubbert *et al.*, 2007). Both extracellular and intracellular antagonists have been identified that spatially and temporally attenuate RAS/MAPK signals (Freeman, 2000). Regulation of RAS/MAPK activation depends on the steady-state level of guanosine triphosphate (GTP)-bound RAS. RAS-GTP levels are negatively regulated by an intrinsic GTPase activity, which is catalyzed by proteins called GTPase activating proteins or RAS-GAPs (Yarwood *et al.*, 2006). In cancer, point mutations cause the loss of one of these two negative feedback mechanisms and prolong the activation of downstream proteins (Downward, 2006).

Correspondence: Benjamin D.-Y. Yu, UCSD School of Medicine, Division of Dermatology, 9500 Gilman Drive, MC-0869, La Jolla, California 92093-0869, USA. byu@ucsd.edu.
[2]These authors contributed equally to this work.

CONFLICT OF INTEREST
The authors state no conflict of interest.

SUPPLEMENTARY MATERIAL
Supplementary material is linked to the online version of the paper at http://www.nature.com/jid

NIH-PA Author Manuscript
NIH-PA Author Manuscript

Recently, activating mutations in RAS- and MAPK-encoding genes have been identified in several human syndromes, including *HRAS* in Costello (Aoki *et al.*, 2005; Schulz *et al.*, 2008), *KRAS* (Schubbert *et al.*, 2006), *BRAF, MEK1*, and *MEK2* in cardiofaciocutaneous (CFC) (Niihori *et al.*, 2006; Rodriguez-Viciana *et al.*, 2006), and *KRAS, PTPN11, RAF1*, and *SOS1* in Noonan syndrome (Schubbert *et al.*, 2006; Roberts *et al.*, 2007; Tartaglia *et al.*, 2007). These syndromes and additional syndromes, neurofibromatosis, LEOPARD, and Legius syndromes, are often referred collectively as RAS/MAPK syndromes, because they share a defect in a common signaling pathway (Rodriguez-Viciana *et al.*, 2006; Brems *et al.*, 2007; Rauen *et al.*, 2008). Three RAS/MAPK syndromes, Costello, CFC, and Noonan syndromes, share many phenotypic similarities, including short stature, craniofacial dysmorphology, cardiomyopathy, and heart valve defects. RAS/MAPK syndromes demonstrate more variability in the degree of neurocognitive impairment, skin manifestations, cancer risk, and type of cancer predisposition (Roberts *et al.*, 2006).

A wide range of ectodermal defects have been noted in RAS/MAPK syndromes, particularly in Costello, CFC, and Noonan syndrome. Costello syndrome patients classically have redundant skin, multiple papillomas, and thickened palms and soles (Hennekam, 2003; Weiss *et al.*, 2004). Progressive hair loss or thinning is reported in Costello (36.4%) and CFC (75.9%) patients, but rarely in Noonan syndrome. Many of the classic features of these syndromes were described prior to the discovery of heterogeneous alleles and genes in RAS/BRAF/MEK, and thus further delineations may be possible. Nevertheless, the phenotypic effects in the skin suggest that developmental processes in skin, brain, and cancer may be uniquely sensitive to RAS activation and its downstream effectors. Recently, mice bearing a strong *Hras*^{G12V} allele have been generated as possible models of Costello syndrome (Schuhmacher *et al.*, 2008; Chen *et al.*, 2009). The *Hras*^{G12V} gain-of-function mice develop cardiomyopathy and papillomas like Costello syndrome patients but apparently lack several many other cutaneous abnormalities.

As noted above, the vast majority of RAS mutations related to Costello syndrome involve mutations in *HRAS*. Mutations in the paralog, *KRAS*, have also been discovered in association with humans with CFC, Costello-like, and Noonan syndromes, although at much lower frequencies (<5%) (Zenker *et al.*, 2007). Differences in paralog gene expression, allele strength, biochemical partners, or early embryonic requirements could contribute to different outcomes of KRAS activation during development and different disease outcomes. To shed light on this question, we investigated the cutaneous response in mice to a strong *Kras*^{G12D} allele. Utilizing a Cre–lox approach to activate *Kras* in different compartments of the ectoderm, we find that *Kras* activation in the ectoderm has multiple effects on nail, hair, and skin defects. The single mutant *Kras*^{G12D} allele induces hyperplasia of limited cell types of the skin, including the basal keratinocytes in the epidermis, sebaceous gland, and outer root sheath (ORS) of the hair follicle. Paradoxically, *Kras*^{G12D} blocks hair cycle activation in the hair follicle but does not directly affect bulge specification or proliferation.

RESULTS

Previous genetic studies in mice have shown that strong activating mutations in *Kras*, such as oncogenic *Kras*^{G12D}, are incompatible with fetal development (Shaw *et al.*, 2007). Similarly, tissue-specific activation of *Kras*^{G12D} in mice, using a keratin 14 (K14)-Cre keratinocyte-specific line to activate KRAS in the ectoderm, also resulted in embryonic lethality (Tuveson *et al.*, 2004). To bypass lethality and to activate KRAS in the mouse epidermis and hair follicle, we used a *Msx2-Cre* transgenic mouse model, which expresses Cre recombinase along the midline epidermis, limb ectoderm of embryos, and the postnatal hair follicle matrix (Sun *et al.*, 2000; Pan *et al.*, 2004). Intercrosses between homozygous Msx2-*Cre* and hemizygous mice carrying a conditional knock-in allele of *Kras*^{G12D}*, Lox-*

Stop-Lox Kras^{G12D} (*LSL-Kras*^{G12D}), generated mice in which *Kras*^{G12D} activation occurs in the epidermis and hair. Importantly, expression of *Kras*^{G12D} remains under the control of its endogenous promoter and thus recapitulates its normal expression pattern, dosage, and regulation (Tuveson *et al.*, 2004).

Msx2-Cre; LSL-Kras^{G12D} (hereafter called Msx2-*Cre; Kras*^{G12D}) mice were born at near expected Mendelian frequency (49%, n = 45/92). Msx2-*Cre; Kras*^{G12D} and control Msx2-*Cre* ("wild type") neonates were grossly equal in size and showed no external signs of congenital malformations. After 1 week of age, Msx2-*Cre; Kras*^{G12D} mice could be recognized by the appearance of redundant skin folds on their face, eyelids, and back (Figure 1a–c). By 2 weeks of age, Msx2-*Cre; Kras*^{G12D} hair became noticeably rough and short compared with wild-type littermates. This abnormal hair appearance persisted into adulthood, and hair loss became apparent after 3 weeks along the midline of the back and throughout the dorsal head (Figure 1b). In older Msx2-*Cre; Kras*^{G12D} mice, the nails also appeared brittle and short (Figure 1d). These cutaneous changes were observed in 100% of adult Msx2-*Cre; Kras*^{G12D} mice (n = 34). None of these phenotypes were observed in their wild-type littermates or in LSL-*Kras*^{G12D} heterozygous mice, which do not have Cre. Spontaneous papillomas were observed in 78% of Msx2-*Cre; Kras*^{G12D} mice as early as 2 weeks of age (Figure 1e and f). Sites of papilloma formation were highly skewed toward non-hair-bearing areas such as the perianal, fore/hindpaw, and head skin. Less than 10% of papillomas developed on back skin, where hair abnormalities were dominant (Supplementary Table S1 online). Histologically, the tumors were consistent with squamous papillomas, and none of the 22 tumors were found to be invasive (Supplementary Figure S1 online). Because of the size of the papillomas (>1 cm), euthanasia of affected animals was performed. These observations indicate that activation of the *Kras*^{G12D} allele in the skin affect the normal homeostasis of the skin and hair and predispose mice to benign papillomas.

Previous work demonstrated that the Msx2-*Cre* transgene is active early in the dorsal ectoderm, as early as E11.5 (prior to hair development). Thus, when Msx2-*Cre* mice are interbred with a Cre-sensitive β-galactosidase reporter in the ROSA locus (*R26R*), more extensive recombination can be detected in the dorsal ectoderm of newborn animals compared with adjacent lateral areas of the skin (Pan *et al.*, 2004). The increased severity along the dorsal midline of Msx2-*Cre; Kras*^{G12D} animals might be because of increased Cre activity in the dorsal skin. We sought to determine the efficiency of recombination at the *Kras* locus based on the relative amount of excision of the intervening LSL-stop cassette, as recombination efficiency can vary between different genetic loci (Akagi *et al.*, 1997). Quantitative PCR revealed 1.7 × more recombination as measured by the relative loss of LSL-stop cassette in dorsal than in lateral whole skin (Supplementary Table S2 online). These findings indicate that like the ROSA locus, recombination and activation of *Kras*^{G12D} is more frequent in the dorsal midline of Msx2-*Cre* mice.

Epidermal response to *Kras* ^{G12D}

The epidermis is a stratified epithelium that is continuously renewed by keratinocyte progenitors located in the basal layer (Blanpain and Fuchs, 2006). Suprabasal keratinocytes are postmitotic and differentiate to form a physical and hydrophobic barrier. To investigate the basis of the Msx2-*Cre; Kras*^{G12D} skin phenotype, we analyzed proliferation and differentiation of the epidermis. The epidermis of Msx2-*Cre; Kras*^{G12D} mice was hypercellular and associated with a dense, hyperproliferative layer of basal keratinocytes (Figure 2a–c and Supplementary Table S2 online). In cultured keratinocytes, proliferation of Msx2-*Cre; Kras*^{G12D} primary keratinocytes was also accelerated and reached a growth plateau of approximately twice the density of wild-type controls before contact inhibition (Figure 2d). Like wild-type littermates, suprabasal keratinocytes of Msx2-*Cre; Kras*^{G12D}

mice were postmitotic, and although the epidermis appeared thicker, Msx2-*Cre; Kras*^{G12D} mice displayed equal numbers of nucleated layers (4 to 5 nucleated layers). Each layer expressed appropriate patterns of differentiation, including K10 and loricrin. These findings indicate that *Kras*^{G12D} primarily affects the basal layer but has little effect on the kinetics of postmitotic differentiation. As an alternative to epidermal thickening as a cause for redundant skin, we considered increased skin surface area as a possible mechanism. To assess the relative change in body surface area, the anterior–posterior lengths of skin biopsies were measured. As skin biopsies varied in size, the contour of the epidermis was normalized to the length of the biopsy base. We found that the relative amount of epidermis produced by Msx2-*Cre; Kras*^{G12D} mice increased by 9.9% more than control littermates (Figure 2e). These results suggest that the redundant skin phenotype in Msx2-*Cre; Kras*^{G12D} mice results from basolateral expansion of basal keratinocytes and the overabundance of body surface area.

Effects of *Kras*^{G12D} on hair growth

Over the next 2 to 3 weeks of age, the Msx2-*Cre; Kras*^{G12D} mice developed progressive hair loss. Significantly, after 3 weeks of age, there was no evidence of new hair growth in affected areas of the Msx2-*Cre; Kras*^{G12D} mice, during a period of the first postnatal hair cycle (Figure 3) (Muller-Rover *et al.*, 2001). A second assay was used to assess new hair growth. After trimming the dorsal hair of mice, all 11 (100%) wild-type littermate mice showed complete hair re-growth in 2 weeks, whereas only 3 of 15 (20%) Msx2-*Cre; Kras*^{G12D} mice had signs of new hair re-growth (Figure 3a). Additionally, to determine if activation of a physiologic hair cycle was merely delayed rather than blocked, we screened for early anagen gene expression (*Shh* mRNA) and hair differentiation (inner root sheath and medulla) over a 30-day window (P18 to P51) in Msx2-*Cre; Kras*^{G12D} mice (Figure 3b–d). In affected areas, none of the 16 Msx2-*Cre; Kras*^{G12D} mice showed signs of anagen growth or hair differentiation. These findings indicate that Msx2-*Cre; Kras*^{G12D} mice have defective activation of the hair cycle.

Histological and immunofluorescent analysis throughout these stages consistently revealed an overgrowth of follicular epithelium resembling ORS cells in Msx2-*Cre; Kras*^{G12D} mice (Figure 4a–c). K14, P63, and SOX9 expression confirm the identity of this tissue (Figure 4d–f and not shown). ORS hyperplasia also persisted during catagen, when hair follicles normally involute and regress (Figure 4b and e). Like wild-type hair follicles, the Msx2-*Cre; Kras*^{G12D} hair follicles were nonproliferative and other cells of the hair follicle appeared to regress normally (not shown). These findings indicate that the Msx2-*Cre; Kras*^{G12D} mice enter catagen and that the *Kras*^{G12D} ORS is relatively resistant to involution. Using two markers of apoptosis, TUNEL and phospho-histone H2A variant X, immunostaining of Msx2-*Cre; Kras*^{G12D} mice revealed lack of cell death in the ORS (Figure 4e, not shown). These findings indicate that during a normal period of scheduled cell death, the ORS of Msx2-*Cre; Kras*^{G12D} mice was resistant to apoptosis.

The tissue that remained after catagen showed varying contributions of SOX9-positive cells in the follicular epithelium, ranging from no contribution to approximately half (Figure 4f). However, the majority of this tissue also expressed high levels of P-cadherin, which is characteristic of an ORS subpopulation called the secondary hair germ (Figure 4f) (Ito *et al.*, 2004; Greco *et al.*, 2009). Failure to initiate a new hair cycle could reflect absence of or defective activation of hair follicle stem cells called bulge cells, which are also derived from ORS tissue (Paus and Cotsarelis, 1999; Tumbar *et al.*, 2004). By staining for several bulge markers (CD34, membrane CCAAT-enhancer-binding protein-α (C/EBPα), and K15), we found that bulge cells were still present in Msx2-*Cre; Kras*^{G12D} mice at all stages of development (Figure 5a–c; not shown) (Bull *et al.*, 2002; Trempus *et al.*, 2003; Morris *et al.*, 2004). Neither Ki-67-positive nor proliferating cell nuclear antigen-positive bulge cells could be detected during any stage of the Msx2-*Cre; Kras*^{G12D} mice; e.g., P16 through P77 (Figure 5c). Thus, *Kras*^{G12D} promotes the expansion of ORS and secondary hair germ-like cells, but does not affect the number or identity of the bulge cells.

To determine whether *Kras*^{G12D} mutations autonomously block cell division in bulge cells to divide or block their differentiation, we utilized a ligand-inducible K15-*CrePR* model to activate *Kras*^{G12D} allele in the bulge cells (Figure 5d). Through the intercross of K15-*CrePR; Kras*^{G12D} and homozygous floxed lacZ (R26R) mice, we generated K15-*CrePR; Kras*^{G12D}; R26R and littermate controls and found no significant difference in the percentage of animals in anagen (Figure 5e). To assess the efficiency of recombination, the percentage of mice with β-galactosidase-positive hair follicles was determined. In all, 83.3% of K15-*CrePR; Kras*^{G12D}; R26R mice demonstrated β-galactosidase-positive hair follicles compared with 90% of K15-*CrePR*; R26R mice (Figure 5f). Moreover, recombination at the Kras locus was confirmed by loss of the LSL-cassette in β-galactosidase-positive hair follicles (Supplementary Table S2 online). Thus, activation of *Kras*^{G12D} in bulge cells did not affect their ability to proliferate and contribute to new hair re-growth.

DISCUSSION

In this study, we investigated the biological response of the skin and hair to activated *Kras* to better understand the developmental consequences of activated RAS. We find that activated *Kras*^{G12D} induces global changes to skin and hair architecture. The resulting phenotype of redundant skin, hair loss, shortened nails, and perianal papillomas in Msx2-*Cre; Kras*^{G12D} mice differed from previous gain-of-function mouse models utilizing either *Kras*^{G12D} or *Hras*^{G12V} alleles. These studies reveal, to our knowledge, previously unreported roles for RAS signaling in the regulation of hair and skin morphogenesis.

Prior to this study, the *Kras*^{G12D} allele had been studied in the context of cutaneous and oral mucosal malignancies through the use of heterotopic promoters, e.g., bi-transgenic *Kras*^{G12D}, tetracycline activated (tet-on) promoter (Vitale-Cross *et al*., 2004), or tissue-specific activation of *Kras*^{G12D} from its endogenous promoter (Tuveson *et al*., 2004; Caulin *et al*., 2007). Heterotopic *Kras*^{G12D}-tet-on activated expression induced histological evidence of epidermal hyperplasia in the skin, oral mucosa, salivary glands, esophagus, stomach and cervix, and various stages of squamous neoplasias, ranging from benign papillomas to metastatic carcinomas. Cre-based studies similarly focused on the neoplastic effects of endogenous *Kras*^{G12D} in the postnatal skin, using topically delivered ligands to activate Cre recombinase. Whereas postnatal activation of *Kras*^{G12D} using a ligand-inducible K5-*CrePR* triggered oral epithelial abnormalities and papillomas (Caulin *et al*., 2007), prenatal activation of *Kras*^{G12D} in the skin ectoderm with K5-*Cre* caused neonatal lethality (Tuveson *et al*., 2004). Thus, many aspects of RAS function during postnatal development remain unknown.

In addition to cancer, RAS/MAPK mutations are also associated with developmental disorders. Developmental consequences in the skin, e.g., redundant skin and hair loss, however, have not been reported in earlier models of *Kras*^{G12D} or *Hras*^{G12V} gain-of-function mice. Lack of developmental or major morphological defects in the skin of these animals could be because of differences in the timing or pattern of RAS activation or in the case of ectopic promoters, nonphysiological levels and regulation of *Kras*^{G12D} gene expression. In the case of *Hras*^{G12V}, in which gain-of-function alleles were introduced into the endogenous locus, differences in the regulation of RAS paralog gene expression or biochemical partners could result in differences in overall phenotype.

The overproduction of skin in Msx2-*Cre; Kras*^{G12D} mice indicate that RAS signals may normally participate in homeostasis of skin production. Skin production as measured by body surface area is normally kept in balance with increasing body size. Similar mechanisms maintain organ size in symmetry with body size (Stern and Emlen, 1999). In the Msx2-*Cre; Kras*^{G12D} mouse, the overall increase in body surface area can be best described phenotypically as excess skin or redundant skin. Wrinkled, sagging, or loose skin, which imply changes in skin laxity, were not observed in the Msx2-*Cre; Kras*^{G12D} mice. Furthermore, changes in elastin and collagen were not observed in our studies (Figure 2e; not shown). Other mouse models with excess skin have been described, which overexpress transforming growth factor-α or fibroblast growth factors (FGF7 and FGF10). In these mice, the skin and basal keratinocytes were also shown to be hyperproliferative (Guo *et al.*, 1993). Unlike the Msx2-*Cre; Kras*^{G12D} mice, overexpressed growth factors caused epidermal thickening and altered patterns of differentiation. At a time when redundant skin first became apparent in the Msx2-*Cre; Kras*^{G12D} mice, the earliest detectable change was hyperplasia of the basal layer of the epithelium. These defects preceded overgrowth of the ORS and sebaceous gland (Figures 2e and 3b and d). Because epidermal thickening and increased stratification were absent in the Msx2-*Cre; Kras*^{G12D} mice, basolateral expansion of the epidermis appears to be the primary cause of redundant skin. Additional studies considering basement membrane production and the apparent anteroposterior directionality of overgrowth are needed to further explore the mechanisms of RAS-mediated body surface area regulation.

Because RAS is regulated by its endogenous promoter in this experimental model, it seems likely that the affected tissues reflect cells and developmental processes that are normally regulated by RAS activation. Endogenous ligands likely to trigger RAS activation in the epidermis include members of the epidermal growth factor and FGF family. Previous studies demonstrate that transforming growth factor-α, an epidermal growth factor family member, is constitutively produced by keratinocytes and functions as an autocrine signal (Guo *et al.*, 1993). FGF ligands such as FGF7 (also called KGF) are instead produced by mesenchyme. Some aspects of the *Kras*^{G12D}-induced epidermal phenotype could be explained by hyperstimulation of both autocrine and paracrine signaling pathways. As overexpression of these ligands produced similar phenotypes, it seems likely that one or more of these growth factors normally have a role in the allometric regulation of skin production. Overexpression of the epidermal growth factor receptor, ErbB2a, also induces hyperplasia of the adnexal structures, including the sebaceous gland (Kiguchi *et al.*, 2000), whereas the *Kras*^{G12D} allele induces hyperplasia of the sebaceous gland and ORS. As *Kras*^{G12D} allele induces a wider spectrum of organ involvement, it is likely that the epidermal, ORS, and sebaceous gland hyperplasia represent the normal signaling domains of all three ligand signals.

A second major phenotype seen in the Msx2-*Cre; Kras*^{G12D} mice was progressive hair loss. Although RAS activation has been implicated in cell cycle arrest in various experimental models (Lin *et al.*, 1998; Courtois-Cox *et al.*, 2006), activation of the *Kras*^{G12D} allele using the bulge Cre line, K15-*CrePR*, was not sufficient to block hair cycling. In addition, *Kras*^{G12D}-recombined cells appeared to be capable of contributing to cells of the hair lineage. The abnormal morphology of Msx2-*Cre; Kras*^{G12D} hair follicles might also prevent the normal activation of bulge and hair germ from anagen stimulatory signals. During normal hair cycle activation, anagen stimulatory signals from the dermal papilla are in close proximity to bulge and hair germ cells (Botchkarev and Paus, 2003). In the Msx2-*Cre; Kras*^{G12D} mice, the persistence of ORS cells during telogen could block this paracrine signaling event. Conversely, paracrine signals, e.g., from abnormal ORS or surrounding tissue, might also affect hair cycle activation or refractoriness (Plikus *et al.*, 2008). As additional progenitor populations have now been identified in the resting hair follicle, additional Cre transgenic approaches will need to be used to determine if the cell autonomous effects of *Kras*^{G12D} differ between different hair progenitor lineages (Snippert *et al.*, 2010).

Last, although KRAS rarely contributes to the human RAS/MAPK syndromes, gross similarities in phenotypes between several cutaneous features of RAS/MAPK syndromes and the Msx2-*Cre; Kras*^{G12D} mice were observed. Loose, redundant skin has been reported in patients with Costello syndrome. Skin biopsies of Costello patients show degenerate elastic fibers (Mori *et al.*, 1996), and thus it is believed that the redundant skin phenotype of Costello syndrome represents elastin defects. The Msx2-*Cre; Kras*^{G12D} mice do not demonstrate loose or sagging skin, which are typical of mice with elastin/collagen abnormalities, e.g., cutis laxa (Nakamura *et al.*, 2002; Suzuki *et al.*, 2003). Furthermore, the Msx2- *Cre; Kras*^{G12D} mice develop redundant skin in the dorsal trunk, rather than dorsal hands and feet, which are commonly affected in Costello syndrome. These differences could be explained by the Cre driver used in our study. Nevertheless, it seems possible that epidermal homeostasis may also contribute to the appearance of redundant skin in Costello syndrome patients. Another phenotype, hair loss, is reported in RAS/MAPK syndromes, in particular CFC (Roberts *et al.*, 2006). Findings from the Msx2-*Cre; Kras*^{G12D} mice suggest that one possible mechanism for hair loss in CFC patients may be hair cycle defects. As mutations in CFC involve BRAF, MEK1, and MEK2, it seems likely that this effector pathway has a significant role in regulating hair cycling. Interestingly, KRAS has been shown to have strong preference toward RAF activation; whereas HRAS has preference for phosphoinositol-3-kinase (Yan *et al.*, 1998). Hair loss in the Msx2-*Cre; Kras*^{G12D} model and normal hair homeostasis in *Hras*^{G12V} gain-of-function mice could reflect effector preferences of KRAS versus HRAS in the hair follicle. The studies highlight the degree of plasticity of the mammalian skin to generate vastly different cutaneous patterns via modulating a single signaling pathway.

MATERIALS AND METHODS

Mouse breeding and genotyping

Mice were genotyped by PCR analysis of tail biopsy DNA using primers as previously described (Tuveson *et al.*, 2004). Msx2-Cre males originated from CD-1 outbred strain, whereas *LSL-Kras*^{G12D} strain was derived from C57BL/6 × 129SvJ. To assess recombination frequency, skin, dissected hair follicles, and papillomas were lysed in tail buffer followed by quantitative PCR to assess the loss of LSL-cassette (LSL-REV 5′-GCTGAACTGAGCGAACAAGTGCAA-3′; LSL-FOR 5′-TTGCCATCGATCCATCTACCACCA-3′). All experiments were performed with approved animal protocols according to the institutional guidelines established by the University of California, San Diego, institutional animal care and use committees.

Histology, *in situ* hybridization, and immunohistochemistry

Immunohistochemical and immunofluorescent stainings were performed on acetone or paraformaldehyde-fixed tissue in conjunction with citrate antigen retrieval. The following antibodies were used for this study: K14 (1:200; Labvision, Fremont, CA), K10 (1:200; Labvision), Loricrin (1:100; gift from Colin Jamora), Ki-67 (1:100; Labvision), AE13 (1:25; Abcam, Cambridge, MA), AE15 (1:100; Santa Cruz Biotechnologies, Santa Cruz, CA), CD34-FITC (1:100; eBioscences, San Diego, CA), p63 4A4 (1:200, Labvision), C/EBP-α (1:100; Santa Cruz Biotechnologies), C/EBP-β (1:500, Santa Cruz Biotechnologies), K15 (1:100; Labvision), and phosphorylated histone H2A variant X (1:100; Cell Signal). *In situ* hybridizations were performed as previously described (Brown *et al.*, 2006). Anti-sense digoxygenin riboprobes were generated according to the manufacturer's instructions (Roche Applied Science, Indianapolis, IN). Shh riboprobes were previously described (Lewis *et al.*, 2001). K17 riboprobes were transcribed from PCR-generated templates from exon 1 (sequences available upon request).

Supplementary Material

Refer to Web version on PubMed Central for supplementary material.

Acknowledgments

We thank Colin Jamora, Bruce Hamilton, and Joseph Gleeson for critiques. This work was supported by grants from the American Skin Association, the University of California Cancer Coordinating Committee, the National Institutes of Health (K08 HD047674 and R01 AR056667), and the California Institute of Regenerative Medicine (RN2-00908-1).

Abbreviations

C/EBPα	CCAAT-enhancer-binding protein-α
CFC	cardiofaciocutaneous
FGF	fibroblast growth factor
GTP	guanosine triphosphate
K15	keratin 15
LSL	Lox-Stop-Lox
MAPK	mitogen-activated protein kinase
ORS	outer root sheath

REFERENCES

Akagi K, Sandig V, Vooijs M, et al. Cre-mediated somatic site-specific recombination in mice. Nucleic Acids Res. 1997; 25:1766–73. [PubMed: 9108159]

Aoki Y, Niihori T, Kawame H, et al. Germline mutations in HRAS proto-oncogene cause Costello syndrome. Nat Genet. 2005; 37:1038–40. [PubMed: 16170316]

Blanpain C, Fuchs E. Epidermal stem cells of the skin. Annu Rev Cell Dev Biol. 2006; 22:339–73. [PubMed: 16824012]

Botchkarev VA, Paus R. Molecular biology of hair morphogenesis: development and cycling. J Exp Zoolog B Mol Dev Evol. 2003; 298:164–80.

Brems H, Chmara M, Sahbatou M, et al. Germline loss-of-function mutations in SPRED1 cause a neurofibromatosis 1-like phenotype. Nat Genet. 2007; 39:1120–6. [PubMed: 17704776]

Brown D, Yu BD, Joza N, et al. Loss of Aif function causes cell death in the mouse embryo, but the temporal progression of patterning is normal. Proc Natl Acad Sci USA. 2006; 103:9918–23. [PubMed: 16788063]

Bull JJ, Muller-Rover S, Chronnell CM, et al. Contrasting expression patterns of CCAAT/enhancer-binding protein transcription factors in the hair follicle and at different stages of the hair growth cycle. J Invest Dermatol. 2002; 118:17–24. [PubMed: 11851871]

Caulin C, Nguyen T, Lang GA, et al. An inducible mouse model for skin cancer reveals distinct roles for gain- and loss-of-function p53 mutations. J Clin Invest. 2007; 117:1893–901. [PubMed: 17607363]

Chen X, Mitsutake N, LaPerle K, et al. Endogenous expression of Hras(G12V) induces developmental defects and neoplasms with copy number imbalances of the oncogene. Proc Natl Acad Sci USA. 2009; 106:7979–84. [PubMed: 19416908]

Courtois-Cox S, Genther Williams SM, Reczek EE, et al. A negative feedback signaling network underlies oncogene-induced senescence. Cancer Cell. 2006; 10:459–72. [PubMed: 17157787]

Downward J. Signal transduction. Prelude to an anniversary for the RAS oncogene. Science. 2006; 314:433–4. [PubMed: 17053139]

Freeman M. Feedback control of intercellular signalling in development. Nature. 2000; 408:313–9. [PubMed: 11099031]

Greco V, Chen T, Rendl M, et al. A two-step mechanism for stem cell activation during hair regeneration. Cell Stem Cell. 2009; 4:155–69. [PubMed: 19200804]

Guo L, Yu QC, Fuchs E. Targeting expression of keratinocyte growth factor to keratinocytes elicits striking changes in epithelial differentiation in transgenic mice. EMBO J. 1993; 12:973–86. [PubMed: 7681397]

Hennekam RC. Costello syndrome: an overview. Am J Med Genet C Semin Med Genet. 2003; 117:42–8. [PubMed: 12561057]

Ito M, Kizawa K, Hamada K, et al. Hair follicle stem cells in the lower bulge form the secondary germ, a biochemically distinct but functionally equivalent progenitor cell population, at the termination of catagen. Differentiation. 2004; 72:548–57. [PubMed: 15617565]

Kiguchi K, Bol D, Carbajal S, et al. Constitutive expression of erbB2 in epidermis of transgenic mice results in epidermal hyperproliferation and spontaneous skin tumor development. Oncogene. 2000; 19:4243–54. [PubMed: 10980598]

Lewis PM, Dunn MP, McMahon JA, et al. Cholesterol modification of sonic hedgehog is required for long-range signaling activity and effective modulation of signaling by Ptc1. Cell. 2001; 105:599–612. [PubMed: 11389830]

Lin AW, Barradas M, Stone JC, et al. Premature senescence involving p53 and p16 is activated in response to constitutive MEK/MAPK mitogenic signaling. Genes Dev. 1998; 12:3008–19. [PubMed: 9765203]

Mori M, Yamagata T, Mori Y, et al. Elastic fiber degeneration in Costello syndrome. Am J Med Genet. 1996; 61:304–9. [PubMed: 8834040]

Morris RJ, Liu Y, Marles L, et al. Capturing and profiling adult hair follicle stem cells. Nat Biotechnol. 2004; 22:411–7. [PubMed: 15024388]

Muller-Rover S, Handjiski B, van der Veen C, et al. A comprehensive guide for the accurate classification of murine hair follicles in distinct hair cycle stages. J Invest Dermatol. 2001; 117:3–15. [PubMed: 11442744]

Nakamura T, Lozano PR, Ikeda Y, et al. Fibulin-5/DANCE is essential for elastogenesis in vivo. Nature. 2002; 415:171–5. [PubMed: 11805835]

Niihori T, Aoki Y, Narumi Y, et al. Germline KRAS and BRAF mutations in cardio-facio-cutaneous syndrome. Nat Genet. 2006; 38:294–6. [PubMed: 16474404]

Pan Y, Lin MH, Tian X, et al. gamma-secretase functions through Notch signaling to maintain skin appendages but is not required for their patterning or initial morphogenesis. Dev Cell. 2004; 7:731–43. [PubMed: 15525534]

Paus R, Cotsarelis G. The biology of hair follicles. N Engl J Med. 1999; 341:491–7. [PubMed: 10441606]

Plikus MV, Mayer JA, de la Cruz D, et al. Cyclic dermal BMP signalling regulates stem cell activation during hair regeneration. Nature. 2008; 451:340–4. [PubMed: 18202659]

Rauen KA, Hefner E, Carrillo K, et al. Molecular aspects, clinical aspects and possible treatment modalities for Costello syndrome: Proceedings from the 1st International Costello Syndrome Research Symposium 2007. Am J Med Genet. 2008; 146A:1205–17. [PubMed: 18412122]

Reuther GW, Der CJ. The Ras branch of small GTPases: Ras family members don't fall far from the tree. Curr Opin Cell Biol. 2000; 12:157–65. [PubMed: 10712923]

Roberts A, Allanson J, Jadico SK, et al. The cardiofaciocutaneous syndrome. J Med Genet. 2006; 43:833–42. [PubMed: 16825433]

Roberts AE, Araki T, Swanson KD, et al. Germline gain-of-function mutations in SOS1 cause Noonan syndrome. Nat Genet. 2007; 39:70–4. [PubMed: 17143285]

Rodriguez-Viciana P, Tetsu O, Tidyman WE, et al. Germline mutations in genes within the MAPK pathway cause cardio-facio-cutaneous syndrome. Science. 2006; 311:1287–90. [PubMed: 16439621]

Schubbert S, Shannon K, Bollag G. Hyperactive Ras in developmental disorders and cancer. Nat Rev Cancer. 2007; 7:295–308. [PubMed: 17384584]

Schubbert S, Zenker M, Rowe SL, et al. Germline KRAS mutations cause Noonan syndrome. Nat Genet. 2006; 38:331–6. [PubMed: 16474405]

Schuhmacher AJ, Guerra C, Sauzeau V, et al. A mouse model for Costello syndrome reveals an Ang II-mediated hypertensive condition. J Clin Invest. 2008; 118:2169–79. [PubMed: 18483625]

Schulz AL, Albrecht B, Arici C, et al. Mutation and phenotypic spectrum in patients with cardio-facio-cutaneous and Costello syndrome. Clin Genet. 2008; 73:62–70. [PubMed: 18042262]

Shaw AT, Meissner A, Dowdle JA, et al. Sprouty-2 regulates oncogenic K-ras in lung development and tumorigenesis. Genes Dev. 2007; 21:694–707. [PubMed: 17369402]

Snippert HJ, Haegebarth A, Kasper M, et al. Lgr6 marks stem cells in the hair follicle that generate all cell lineages of the skin. Science. 2010; 327:1385–9. [PubMed: 20223988]

Stern DL, Emlen DJ. The developmental basis for allometry in insects. Development (Cambridge, UK). 1999; 126:1091–101.

Sun X, Lewandoski M, Meyers EN, et al. Conditional inactivation of Fgf4 reveals complexity of signalling during limb bud development. Nat Genet. 2000; 25:83–6. [PubMed: 10802662]

Suzuki A, Itami S, Ohishi M, et al. Keratinocyte-specific Pten deficiency results in epidermal hyperplasia, accelerated hair follicle morphogenesis and tumor formation. Cancer Res. 2003; 63:674–81. [PubMed: 12566313]

Tartaglia M, Pennacchio LA, Zhao C, et al. Gain-of-function SOS1 mutations cause a distinctive form of Noonan syndrome. Nat Genet. 2007; 39:75–9. [PubMed: 17143282]

Trempus CS, Morris RJ, Bortner CD, et al. Enrichment for living murine keratinocytes from the hair follicle bulge with the cell surface marker CD34. J Invest Dermatol. 2003; 120:501–11. [PubMed: 12648211]

Tumbar T, Guasch G, Greco V, et al. Defining the epithelial stem cell niche in skin. Science. 2004; 303:359–63. [PubMed: 14671312]

Tuveson DA, Shaw AT, Willis NA, et al. Endogenous oncogenic K-ras(G12D) stimulates proliferation and widespread neoplastic and developmental defects. Cancer Cell. 2004; 5:375–87. [PubMed: 15093544]

Vitale-Cross L, Amornphimoltham P, Fisher G, et al. Conditional expression of K-ras in an epithelial compartment that includes the stem cells is sufficient to promote squamous cell carcinogenesis. Cancer Res. 2004; 64:8804–7. [PubMed: 15604235]

Weiss G, Confino Y, Shemer A, et al. Cutaneous manifestations in the cardiofaciocutaneous syndrome, a variant of the classical Noonan syndrome. Report of a case and review of the literature. J Eur Acad Dermatol Venereol. 2004; 18:324–7. [PubMed: 15096145]

Yan J, Roy S, Apolloni A, et al. Ras isoforms vary in their ability to activate Raf-1 and phosphoinositide 3-kinase. J Biol Chem. 1998; 273:24052–6. [PubMed: 9727023]

Yarwood S, Bouyoucef-Cherchalli D, Cullen PJ, et al. The GAP1 family of GTPase-activating proteins: spatial and temporal regulators of small GTPase signalling. Biochem Soc Trans. 2006; 34:846–50. [PubMed: 17052212]

Zenker M, Lehmann K, Schulz AL, et al. Expansion of the genotypic and phenotypic spectrum in patients with KRAS germline mutations. J Med Genet. 2007; 44:131–5. [PubMed: 17056636]

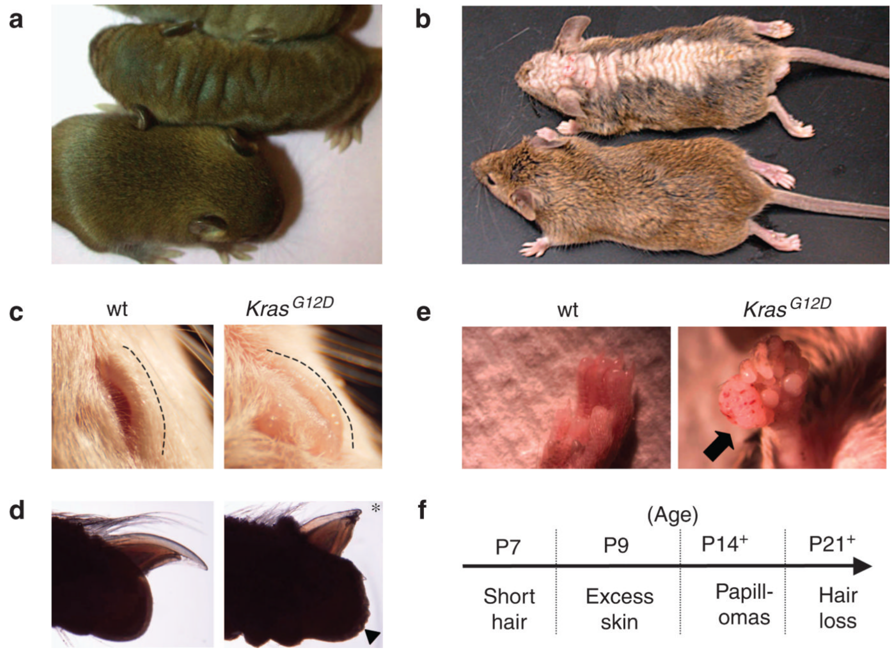

Figure 1. Overview of cutaneous defects in Msx2-*Cre; Kras*^{G12D} mice

(**a**) The 10-day-old and (**b**) 9-week-old Msx2-*Cre; Kras*^{G12D} (*Kras*^{G12D}) and control (wt) littermates demonstrate redundant skin and hair loss phenotypes. (**c**) Thickened eyelids and (**d**) shortened nails of Msx2-*Cre; Kras*^{G12D} and wild-type littermate mice. Asterisk denotes abnormal short nail and arrowhead identifies coarse volar skin surface of Msx2-*Cre; Kras*^{G12D} mice. (**e**) Papilloma on forepaw of Msx2-*Cre; Kras*^{G12D} versus wild-type littermate. (**f**) Age of onset of progressive cutaneous phenotypes in Msx2-*Cre; Kras*^{G12D} mice.

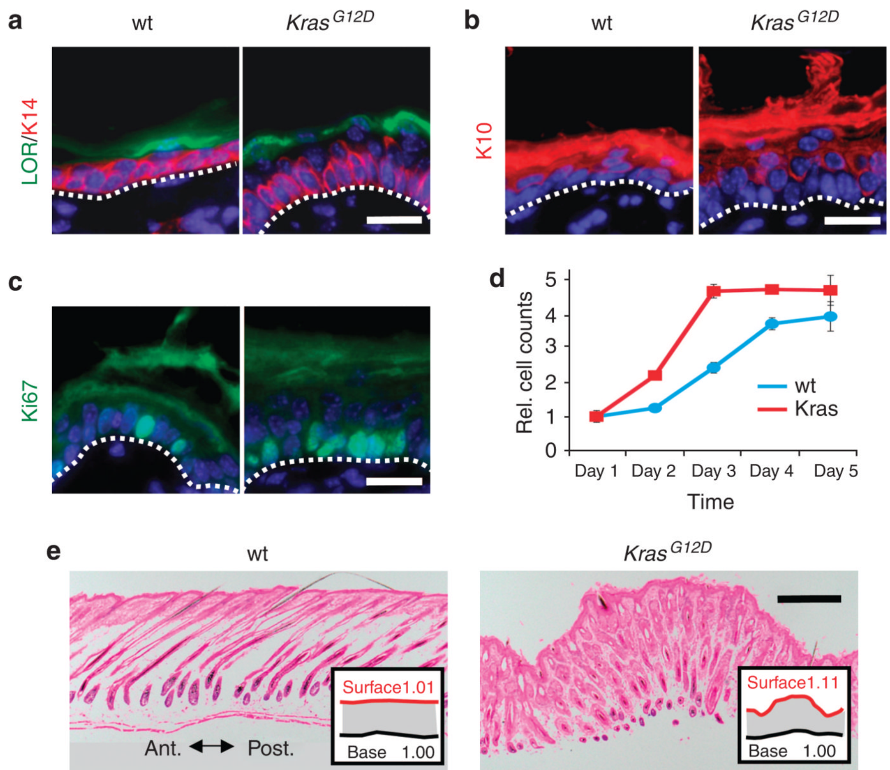

Figure 2. Ectodermal activation of *Kras*^{G12D} causes excess epidermis production

(**a**) Keratin 14 (K14)-positive basal keratinocytes in postnatal day 4 (P4) Msx2-*Cre; Kras*^{G12D} and littermate mice. Loricrin (LOR) identifies uppermost differentiated granular layer of the epidermis. (**b**) Suprabasal differentiation (K10) and number of stratified layers are similar between Msx2-*Cre; Kras*^{G12D} and wild-type mice. (**c**) Ki-67 immunofluorescence in basal epidermis of Msx2-*Cre; Kras*^{G12D} mice. (**d**) Proliferation assay of P2 wild-type (blue) and Msx2-*Cre; Kras*^{G12D} (red) keratinocytes reveals increased growth and density. (**e**) Histological sections demonstrate surface contour of P10 wild-type and Msx2-*Cre; Kras*^{G12D} mice. Length of the surface contour (red) is normalized to length of biopsy (black). White scale bar = 20 μm; black scale bar = 200 μm.

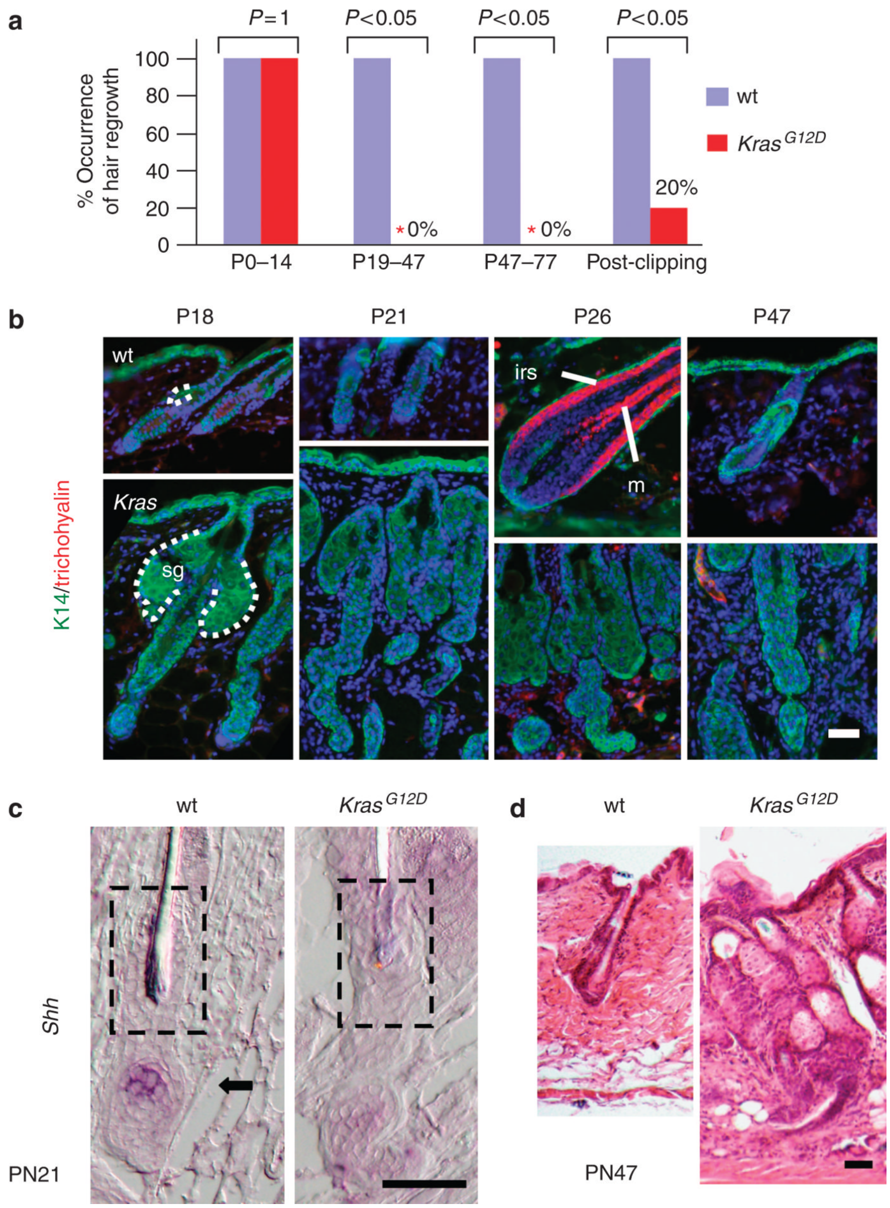

Figure 3. Screen for hair cycle activation and maturation in Msx2-*Cre; Kras*^{G12D} mice

(**a**) Hair growth in wild-type versus Msx2-*Cre; Kras*^{G12D} animals at different stages of development. (**b**) Immunofluorescence for hair differentiation markers, IRS (irs) and medulla (m), using anti-trichohyalin antibody and keratin 14 (K14), a marker for outer root sheath (ORS), sebaceous gland (sg), and basal epidermal marker. Positive trichohyalin staining in postnatal day 26 (P26) wild type demonstrates normal timing of hair growth and differentiation. (**c**) RNA *in situ* hybridization for *Shh* RNA (*arrow*) reveals activation in wild-type early anagen hair follicle. (**d**) Hematoxylin stain of telogen hair follicle of wild-type mice compared with abnormal persistence of basaloid keratinocytes. White and black scale bars = 50 μm.

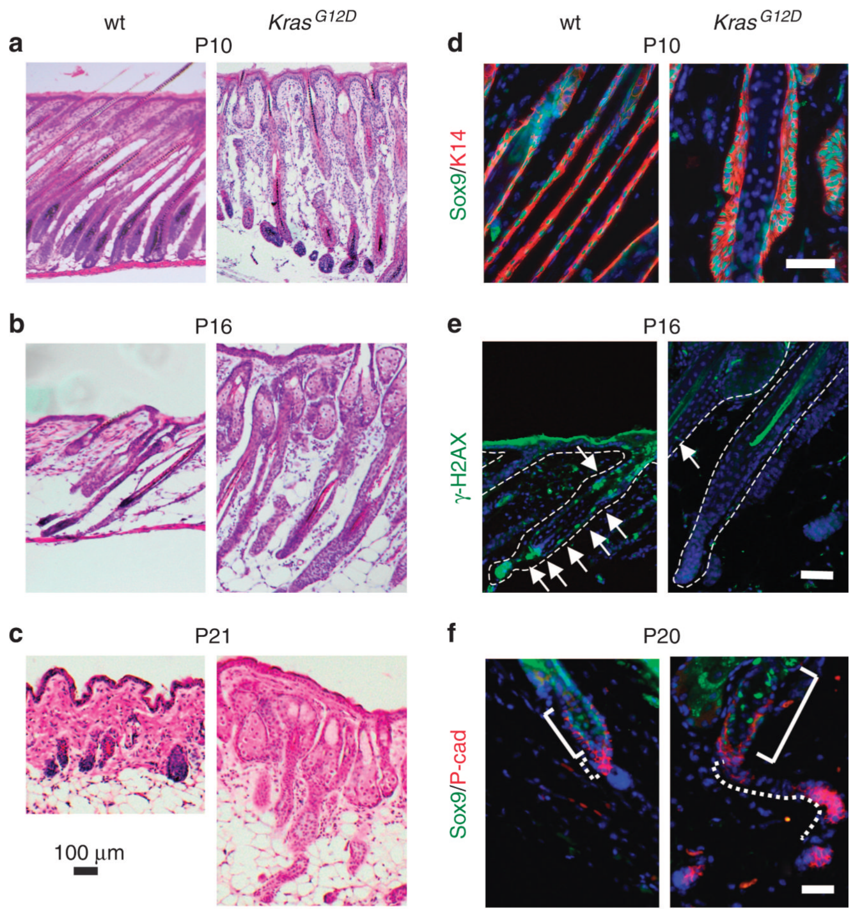

Figure 4. Outer root sheath (ORS) analysis in Msx2-*Cre; Kras*^{G12D} mice

(**a–c**) Histology of postnatal day 10 (P10; anagen), P16 (catagen), P21 (early anagen) of wild-type and Msx2-*Cre; Kras*^{G12D} hair follicles. (**d**) P10 analysis of hyperplastic ORS in Msx2-*Cre; Kras*^{G12D} mice reveals irregular patterns of keratin 14 (K14)-positive, Sox9-positive ORS growth. (**e**) Apoptosis of P16 wild-type and Msx2-*Cre; Kras*^{G12D} hair follicles as detected by phosphorylated histone H2A variant X (H2AX) staining (green, arrows). (**f**) Immunofluorescence reveals persistent and abundant secondary hair germ and ORS in telogen of Msx2-*Cre; Kras*^{G12D} mice. Solid bracket indicates SOX9-positive cells in the region of the bulge. Dotted line indicates boundary of secondary hair germ in wild-type and of remnant ORS tissue in Msx2-*Cre; Kras*^{G12D} mice. Black scale bar (**a–c**) = 100 μm; white scale bar (**d–f**) = 50 μm.

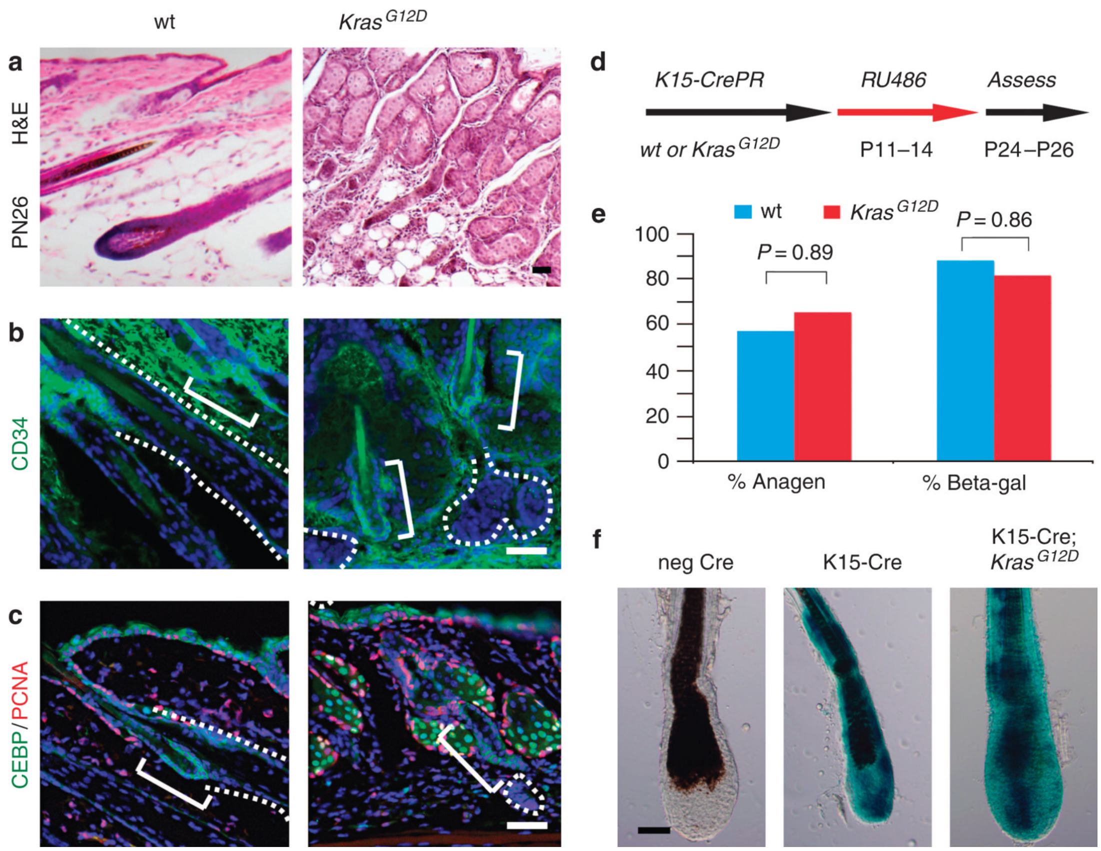

Figure 5. Bulge analysis in Msx2-*Cre; Kras*^{G12D} and K15-*CrePR; Kras*^{G12D} mice

(**a**) Histology of wild-type and Msx2-*Cre; Kras*^{G12D} hair follicles at postnatal day 26 (P26). (**b**) CD34 staining identifies bulge cells in P27 wild-type and Msx2-*Cre; Kras*^{G12D} hair follicles (solid bracket). Contours of follicular tissue are indicated by dotted lines. (**c**) A second bulge marker, CCAAT-enhancer-binding protein-α (C/EBPα) staining at P26, reveals presence of bulge cells in both wild-type and Msx2-*Cre; Kras*^{G12D} mice. (**d**) Schematic of RU486 ligand induced bulge-specific recombination of *Kras*^{G12D} from P11 to P14. (**e**) Percent anagen or β-galactosidase-positive recombination between P24 and P26 of K15-*CrePR; Kras*^{G12D} mice. (**f**) β-galactosidase staining of K15-*CrePR* P26 hair follicles exhibiting fate of recombined cells of wild-type and *Kras*^{G12D} mice. Scale bars = 50 μm.